Equivalent Circuit Model for Designing of Jerusalem Cross-Based Artificial Magnetic Conductors

Mirshahram HOSSEINIPANAH, Qun WU

School of Electronics and Information Engineering, Harbin Institute of Technology,
92 Xidazhi Street, 150001 Harbin, Heilongjiang, P.R. China, POBOX 341

mirshahram@gmail.com, qwu@hit.edu.cn

Abstract. *This paper introduces an equivalent circuit model to estimate the resonant frequency and reflection phase of Jerusalem cross-based artificial magnetic conductor (JC-AMC) structures for waves normally incident on the structure. The JC-AMC structure is composed of an array of Jerusalem cross-shaped frequency selective surfaces (JC-FSSs) printed on a metal-backed dielectric slab without vias. This approach is based on the coupled microstrip lines and transmission line theories. Analytical expressions for the resonant frequency and reflection phase resulting from our model are thoroughly verified by full-wave simulations for different samples reported in the open literature. A comprehensive parametric study of the design parameters of JC-AMC structure and the influence of these parameters on the reflection phase properties are presented. This model can easily be extended to complex-shaped AMCs.*

Keywords

Artificial magnetic conductor, electromagnetic bandgap, high-impedance surface, Jerusalem crosses, equivalent circuit model.

1. Introduction

Artificial magnetic conductor (AMC) structures are characterized by the frequencies where the reflection coefficient phase is zero. This property was introduced by Sievenpiper et al., for mushroom structure, which consists of an array of metal plates on a grounded dielectric slab where the plates are connected to the ground through vias [1, 2]. Research on AMC structures can be roughly split into four categories: designing, applications, modification and modeling. Generally, modeling of AMC structure has been performed by analytical and numerical methods. The numerical method consumes considerable time and computational resources. However, the numerical methods are not restricted to geometry of structures and they can provide accurate results. On the other hand the analytical models thrive, for they are easy to use and yield better insight into physical phenomena. Moreover, the characteristics of the AMC structure can be estimated by an ana-lytical model, and then these estimations can be used by a numerical method to obtain final and accurate results with less design effort.

For many years frequency selective surfaces (FSSs) have been used in antenna systems and microwave devices. Recently, with the advent of AMC structure and its unique properties, Jerusalem cross-shaped FSS (JC-FSS) has also entered the AMC domain. AMC miniaturization is practically equivalent to the decreasing of the resonant frequency of a structure with a given unit cell size [3]. In [4], it was proposed the resonant frequency of a mushroom structure can be decreased by using an array of FSSs instead of metal patches. Furthermore, for a plane wave at normal incidence to the AMC structure, removing the vias has little effect on the in-phase reflection properties and reflection-phase characteristic [5].

A JC-AMC structure can be obtained by utilizing a JC-FSS on top of a grounded dielectric slab without vias (see Fig. 1). In the following, an equivalent circuit model for the JC-AMC structure is proposed. This model is based on coupled microstrip lines and transmission line theories. A comprehensive parametric study involving various design parameters of JC-AMC structure and the effect of these parameters on the reflection phase feature is presented. In order to find out the accuracy of the model, many reported samples, in the open litrerature, are designed with the model, and their results are verified by full-wave numerical simulation (using CST Microwave Studio package). In this paper, a single unit cell of the JC-AMC surface with periodic boundary conditions (PBC) on four sides is simulated to model an infinite surface.

2. Equivalent Circuit Model

Consider a JC-FSS element, located at the interface of a metal-backed dielectric slab without vias. The perspective of AMC unit cell is shown in Fig. 1 and the dimensions of JC-FSS are depicted in Fig. 2. The JC-FSS elements and ground plane are assumed to be perfectly conducting. When the period is small compared to the wavelength of interest, the characteristics of the artificial magnetic conductor can be explained using an effective surface impedance model as shown in Fig. 3.
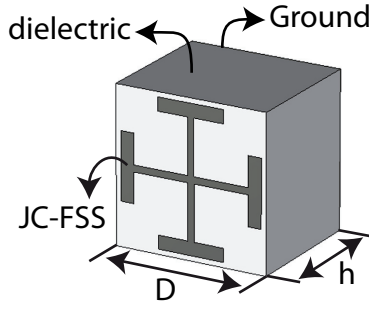
Fig. 1. The perspective of Jerusalem cross-based AMC unit cell.
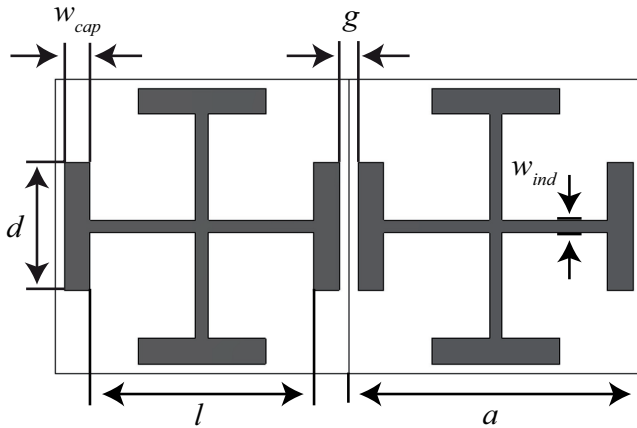
Fig. 2. The geometry and dimensions of Jerusalem cross FSS.
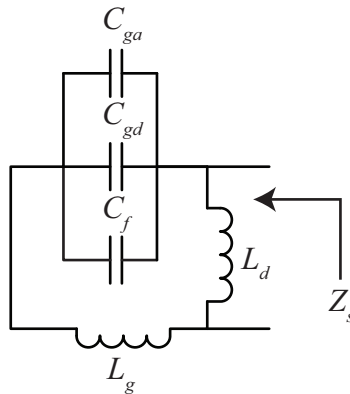
Fig. 3. The equivalent circuit model of AMC.

For the AMC structures, the surface impedance (Z_S) plays an important role to determine the resonant frequency and the phase of reflection coefficient. The surface impedance, in terms of the transmission-line approach can be expressed as a parallel connection of JC-FSS impedance (Z_g) and the surface impedance of a grounded dielectric slab (Z_d) [6]. Therefore, in Fig. 3, the surface impedance can be written as:

$$Z_S(\omega) = Z_g \parallel Z_d = \frac{j\omega L_d (1 - \omega^2 L_g (C_{ga} + C_{gd} + C_f))}{1 - \omega^2 (C_{ga} + C_{gd} + C_f)(L_d + L_g)}. \quad (1)$$

where ω is angular frequency. The inductances of grounded dielectric slab and JC-FSS grid are expressed by L_d and L_g respectively. The capacitances which are formed

in the gap (as specified by g in Fig. 2) between adjacent JC-FSS are shown by C_{ga}, C_{gd} and C_f. It was shown that the error related with the approximate formula (1) is very small whenever the influence of the FSS to Z_d (and vice versa) is negligible. For the special case of mushroom structure, it was shown that when the grid period is not very large compared to the thickness of AMC, the isolation is sufficient [7]. On the other hand in [6] it was proposed that, for the JC-based AMC without vias, the largest width of JC-FSS (w_{cap} or w_{ind}) should be used instead of grid period, as a rule of thumb it can be written as: Max(w_{cap}, w_{ind})/h < 2. When the denominator of (1) equals zero the resonant frequency can be obtained by

$$f_r = \frac{1}{2\pi\sqrt{(C_{ga} + C_{gd} + C_f)(L_g + L_d)}}. \quad (2)$$

At the resonant frequency the surface impedance is very high and the reflection phase coefficient is zero. In the following, the calculation methods of L_g, L_d, C_{ga}, C_{gd}, and C_f are explained. To facilitate this, closed-form formula of characteristic impedance (Z_0) and effective permittivity (ε_{re}) are used which have been reported by Wheeler and Schneider. The maximum relative error in ε_{re} and Z_0 is less than 1%. Z_0 is expressed by [8]

$$Z_0 = \begin{cases} \frac{\eta}{2\pi\sqrt{\varepsilon_{re}}} \ln\left\{\frac{8h}{w} + 0.25\frac{w}{h}\right\} & , \frac{w}{h} \leq 1 \\ \frac{\eta}{\sqrt{\varepsilon_{re}}} \left\{\frac{w}{h} + 1.393 + 0.667\ln\left(\frac{w}{h} + 1.444\right)\right\}^{-1} & , \frac{w}{h} \geq 1 \end{cases} \quad (3)$$

where η is impedance of free space, h is the thickness of dielectric slab, w is width of microstrip line and the effective dielectric constant can be calculated by [8]

$$\varepsilon_{re} = \frac{\varepsilon_r + 1}{2} + \frac{\varepsilon_r - 1}{2} F\left(\frac{w}{h}\right) \quad (4)$$

where

$$F\left(\frac{w}{h}\right) = \begin{cases} \left(1 + \frac{12h}{w}\right)^{-\frac{1}{2}} + 0.041\left(1 - \frac{w}{h}\right)^2 & , \frac{w}{h} \leq 1 \\ \left(1 + \frac{12h}{w}\right)^{-\frac{1}{2}} & , \frac{w}{h} \geq 1 \end{cases} \quad (5)$$

In order to calculate the capacitances and inductances of equivalent circuit model, we decompose the JC-FSS into two components: capacitive component and inductive components. These components are discussed more detail in below.

2.1 Grid Capacitance of a JC-FSS

The grid capacitance is formed in the gap between two adjacent capacitive components. In Fig. 2 the capacitive components are specified by the length of d and the width of w_{cap}. The combination of two parallel capacitive components with the gap distance of g at the surface of metal-backed dielectric slab is similar to the structure of

coupled microstrip lines. Therefore, we used the formula of coupled-line microstrip to obtain the value of JC-FSS capacitances. To this aim the value of C_{ga} which describes the gap capacitance in air can be obtained by [9]:

$$C_{ga} = 2\varepsilon_0\varepsilon_{re}\frac{K(k)}{K'(k)}d \qquad (6)$$

where ε_0 is permittivity of free space,

$$\frac{K(k)}{K'(k)} = \begin{cases} \dfrac{1}{\pi}\ln\left\{2\dfrac{1+\sqrt{k}}{1-\sqrt{k}}\right\} & ,\, 0.707 \leq k \leq 1 \\[4mm] \dfrac{\pi}{\ln\left[2\dfrac{1+\sqrt{k'}}{1-\sqrt{k'}}\right]} & ,\, 0 \leq k \leq 0.707 \end{cases} \qquad (7)$$

$$k = \tan^2\left(\frac{a\pi}{4b}\right),\ a = \frac{w_{cap}}{2},\ b = \frac{(w_{cap}+g)}{2} \text{ and } k' = \sqrt{1-k^2} . \quad (8)$$

The effective permittivity can be calculated by (4) when w is replaced by the width of capacitive component (w_{cap}). The second capacitance (C_f) is the fringe capacitance at the outer edge of the strip and is obtained by the following expression [9]

$$C_f = \frac{1}{2}\left(\frac{\sqrt{\varepsilon_{re}}}{cZ_0} - \frac{\varepsilon_0\varepsilon_r w_{cap}}{h}\right) \qquad (9)$$

where c is velocity of light in free space and Z_0 is obtained by (3) for a strip width of w_{cap}. Over the following range of parameters, the values are found to be accurate to within 3%:

$$0.1 \leq \frac{w_{cap}}{h} \leq 10,\ \ 0.1 \leq \frac{g}{h} \leq 5 \text{ and } 1 \leq \varepsilon_r \leq 18 .$$

The last capacitance (C_{gd}) represents the capacitance value due to the electric flux in the dielectric region. C_{gd} is evaluated by [9]:

$$C_{gd} = \frac{\varepsilon_0\varepsilon_r}{\pi}\ln\coth\left(\frac{\pi g}{4h}\right) + 0.65C_f\left\{\frac{0.02h\sqrt{\varepsilon_r}}{g} + \left(1-\frac{1}{\varepsilon_r^2}\right)\right\} . \quad (10)$$

Using equations (6), (9) and (10) predict accurate values for capacitive component of JC-AMC.

2.2 Grid Inductance of JC-FSS

The inductive component (L_g) of JC-FSS is specified in Fig. 2 by the length of l and the width of w_{ind}. Using microstrip transmission-line theory we can approximate the inductive component by the following formula [9]:

$$L_g = \frac{Z_0\sqrt{\varepsilon_{re}}}{c}l \qquad (11)$$

where Z_0 and ε_{re} can be obtained by (3) and (4) when the width of strips is replaced by w_{ind}. It is noted that, (11) is valid only when l is much smaller than the wavelength of interest.

2.3 Inductance of Grounded Dielectric Slab

For an incident wave normal to the surface of the JC-AMC the impedance of metal-backed dielectric slab with the thickness of h can be expressed by [7]

$$Z_d = \left(\frac{j\eta}{\sqrt{\varepsilon_r}}\right)\tan kh \qquad (12)$$

where $\eta = \sqrt{\mu_0/\varepsilon_0}$ is the impedance of free space, ε_r is relative permittivity of dielectric slab and k is wave number of refracted wave which can be written as:

$$k = \omega\sqrt{\varepsilon_r\varepsilon_0\mu_0} . \qquad (13)$$

According to assumption for the effective surface impedance model all of the dimensions including the thickness of substrate are much smaller than wavelength of interest ($k.h \ll 1$) then (12) can be turned to the frequency-independent equation presented in [2]

$$L_d = \mu_0 h . \qquad (14)$$

3. Parametric Study

The reflection phase of the JC-AMC surface is mainly determined by seven parameters (see Figs. 1 and 2): capacitive components length (d), capacitive components width (w_{cap}), gap width (g), substrate permittivity (ε_r), inductive components length (l), inductive components width (w_{ind}) and substrate thickness (h). In the following, the effects of these parameters on the reflection phase and the resonant frequency of JC-AMC structure are discussed. It is noted that, to study the effect of one parameter, the other parameters should not be changed. In order to estimate the phase of reflection coefficient for a normally incident wave the following expression is used [5]:

$$\Phi = \operatorname{Im}\left[\ln\left(\frac{Z_s - \eta}{Z_s + \eta}\right)\right] \qquad (16)$$

where Z_S is calculated by (1).

Consider a JC-AMC structure with the following parameters (see Figs. 1 and 2):

$$d = 3.5 \text{ mm},\ w_{cap} = 0.1 \text{ mm},\ g = 0.4 \text{ mm},\ \varepsilon_r = 2.2,$$
$$l = 4 \text{ mm},\ w_{ind} = 0.1 \text{ mm, and } h = 1 \text{ mm}. \qquad (15)$$

The reflection phases resulting from the equivalent circuit model and the numerical simulation of this structure are shown in Fig. 4. The resonant frequencies resulting from proposed model and numerical simulation are 9.93 GHz and 9.74 GHz respectively. Accuracy comparison between the equivalent circuit model and simulation is carried out in terms of the relative error that can be obtained by:

$$Error\% = \left|\frac{f_r^{Equivalent\ Circuit\ Model} - f_r^{Simulation}}{f_r^{Simulation}}\right| \times 100. \quad (16)$$

Accordingly, the relative error of resonant frequency for equivalent circuit model is 1.9%.
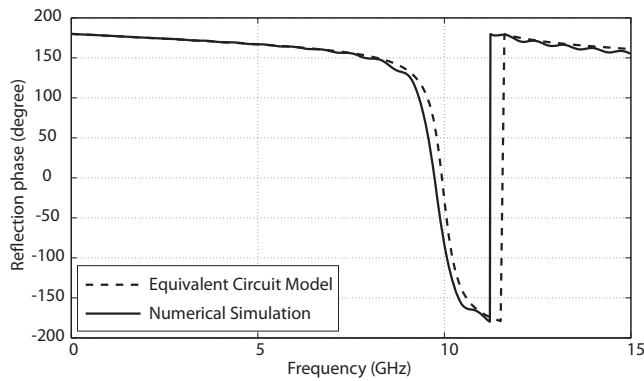
Fig. 4. The reflection phases plotted by equivalent circuit model and numerical model.

3.1 Capacitive Components Length Effect

The length of capacitive components plays an important role in determining the resonant frequency and relative bandwidth. The relative bandwidth defined as the frequency range in which the phase of reflected wave varies in the range ±90°. In (15) the length of capacitive component changes to 2 mm and the other parameters are kept the same. For this structure, the reflection phases resulting from proposed model and numerical simulation are shown in Fig. 5. Comparing the results of Fig. 5 with those of Fig. 4, we can see that, when the length of capacitive component is decreased, the resonant frequency position and its relative bandwidth increase. The resonant frequencies from equivalent circuit model and numerical simulation are 13.14 GHz and 12.40 GHz respectively. The relative error of predicted resonant frequency is 5.9%.
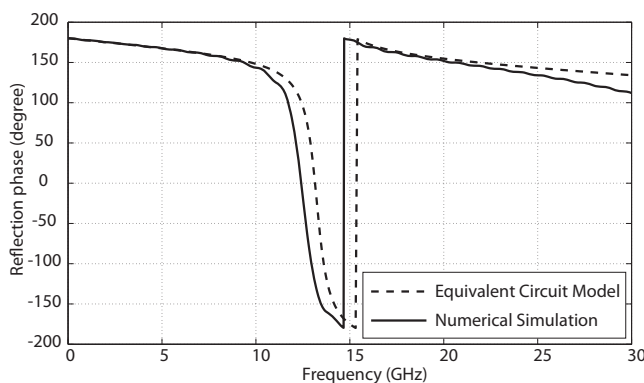
Fig. 5. The effect of capacitive component length.

3.2 Effect of Capacitive Components Width

Variation of capacitive component width effects on the frequency band of JC-AMC surface. During this investigation, the width of capacitive components is changed to 0.5 mm and the other parameters are kept the same as in (15). Fig. 6 displays the reflection phases with numerical method and equivalent circuit model. Comparing Fig. 6

with Fig. 4 shows that, as the widths increases, both the resonant frequency and the bandwidth decreases. Using numerical simulation, the resonant frequency of 8.22 GHz is obtained and the value of that equals to 8.6 GHz using equivalent circuit model. The relative error of predicted resonant frequency is 4.62%.
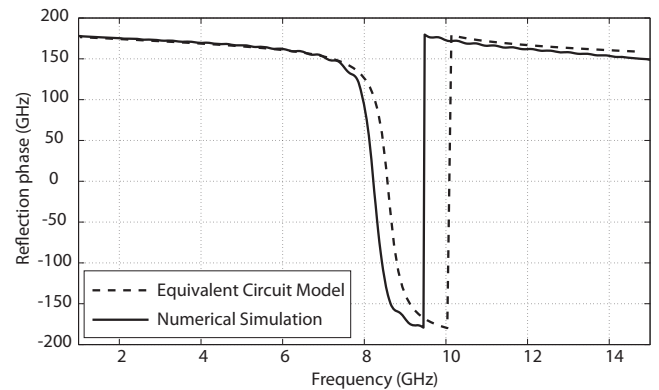
Fig. 6. The effect of capacitive component width.

3.3 Gap Width Effect

The gap width is the distance between two adjacent capacitive components. Variation of the gap width changes the resonant frequency of JC-AMC surface. The structure analyzed here has the same parameters as (15) and the gap width is changed to 0.2 mm. Fig. 7 shows the reflection phases plotted by equivalent circuit model and numerical simulation. Comparing the results of Fig. 7 with those of Fig. 4 illustrates that, when the gap width is decreased, both the resonant frequency and bandwidth decreases. The resonant frequency of 8.26 GHz is predicted by equivalent circuit model and the value of that is obtained 8.76 GHz using numerical method. The relative error of predicted resonant frequency is 5.7%.
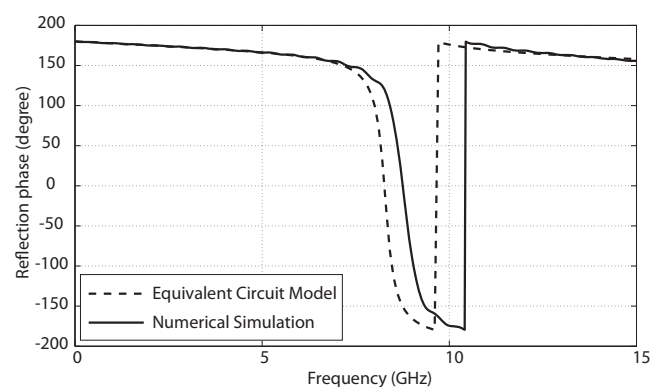
Fig. 7. The effect of gap width.

3.4 Effect of Substrate Permittivity

The relative permittivity of dielectric layer is an effective parameter, which is used to tune the resonant frequency. The structure has the same parameters as (15), except that the permittivity is changed to 5. The reflection

phases are plotted in Fig. 8 using equivalent circuit model and numerical method. Comparison between Fig. 8 and Fig. 4 shows that, when the permittivity of substrate is increased, the resonant frequency and bandwidth decrease. In Fig. 8 the resonant frequency, resulting from simulation is 7.06 GHz and the predicted resonant frequency using equivalent circuit model is 6.9 GHz. The relative error of predicted resonant frequency is 2.26%.
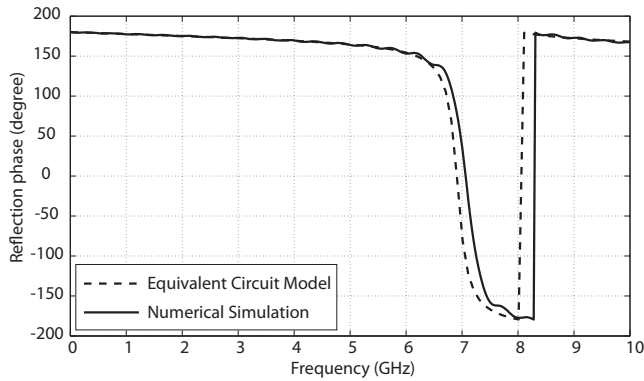
Fig. 8.   The effect of substrate permittivity.

3.5 Effect of Inductive Component Length

The resonant frequency and the bandwidth are affected by variation of the inductive component length. In the following, the length of inductive component varies to 6 mm and the other parameters are the same as in (15). The reflection phases with both numerical method and equivalent circuit model are shown in Fig. 9. Comparing the results of Fig. 8 with Fig. 4 shows that, as the inductive component length increases, both the resonant frequency and the bandwidth decreases. The predicted resonant frequency resulting from equivalent circuit model is 8.49 GH and the resonant frequency of 7.94 GHz is obtained by numerical method. The relative error of predicted resonant frequency equals to 6.9%.
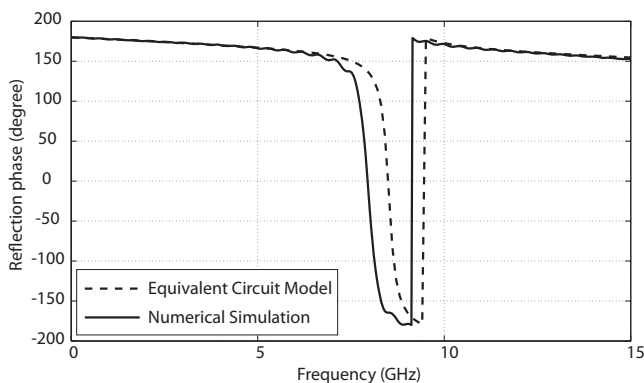
Fig. 9.   The effect of inductive component length.

3.6 Width of Inductive Component Effect

The JC-AMC structure analyzed here has the same parameters as (15), except that the width of inductive component is changed to 0.5 mm. In Fig. 10, the reflection

phases are plotted by numerical method and equivalent circuit model. Comparing the results of Fig. 10 with those of Fig. 4 illustrates that, when the width of inductive component is increased the resonant frequency and bandwidth increase. The resonant frequency obtained by numerical method is 11.48 GHz and the predicted resonant frequency by equivalent circuit model is 11.62 GHz. The relative error for predicted resonant frequency is 1.2%.
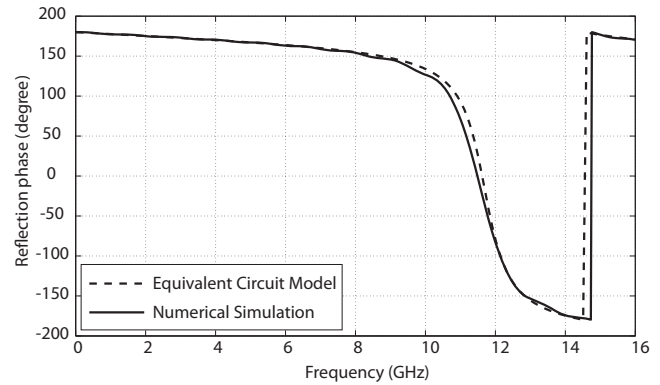
Fig. 10. The effect of inductive component width.

3.7 Substrate Thickness Effect

Generally, in wireless communication devices, thin AMC surfaces are desired. The thickness of substrate has an important role in determining the frequency band. In (15), only the substrate thickness changes to 1.3 mm. Fig. 11 displays the reflection phases resulting from numerical method and proposed model. Comparison between Fig. 11 and Fig. 4 shows that, when the thickness of substrate is increased, the resonant frequency decreases and at the same time the bandwidth increases. The predicted resonant frequency is 8.84 GHz. The resonant frequency of 9.3 GHz is obtained by numerical method. The relative error of prediction is 4.9%.
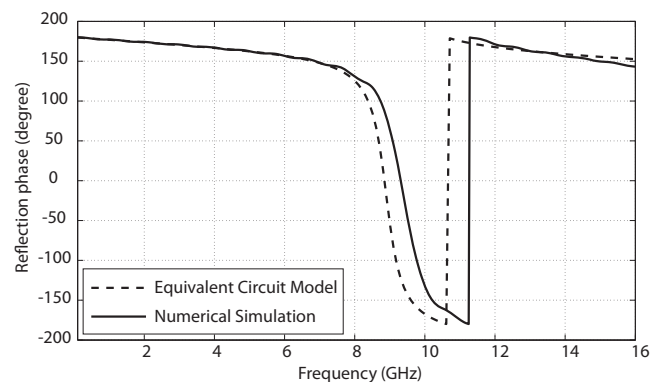
Fig. 11. The effect of substrate thickness.

4. Model Validation

In order to validate the proposed model, many reported samples in open literature were designed by proposed model and were simulated by CST Microwave

Samples	One	Two	Three	Four	Five	Six	Seven	Eight	Nine
ε_r	6	2.7	13	7	10.2	1	1	1	2.2
h	5	6	1	0.5	0.9	1	1	10	0.5
g	0.25	0.1	0.1	0.1	0.11	0.1	0.1	2	0.1
l	5	3.5	1	2	1.29	2	1	27	6.4
w_{ind}	0.3	0.2	0.1	0.5	0.32	0.1	0.1	1	0.5
d	1.7	2	0.8	1.5	0.64	1.5	0.8	25	4
w_{cap}	0.6	0.2	0.5	0.5	0.32	0.5	0.5	1	0.5
f_r^{Model}	3.68	4.63	8.88	12.03	12.6	16.79	27.19	1.59	6.9
f_r^{CST}	3.78	4.64	9.5	11.46	13.2	16.14	26.22	1.62	7.05
$Error\%$	2.64	0.2	6.52	4.97	4.54	4	3.69	1.8	2.1

Tab. 1. The comparison between equivalent circuit model and numerical simulation for nine samples.

Studio. The results were rendered in Tab. 1. Accuracy comparison between the equivalent circuit model and numerical simulation is presented in the last row of the table in terms of error i.e. relative error. In [7] the second sample was analyzed using Ansoft's HFSS package and our model accurately predicts the resonant frequency and reflection phase diagram of this structure. As shown in Fig. 12 the simulation result verifies the prediction of the model. Comparing the results of our model with reported model in [7] shows that, when an incident wave is normal to the surface of JC-AMC structure, the resonant frequency and reflection phase can be predicted more accurate using our model.
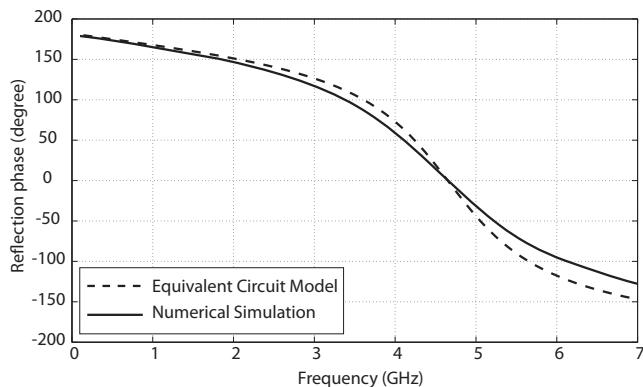
Fig. 12. The reflection phase diagram of sample 2 resulting from proposed model and numerical simulation.

The third, fifth and seventh samples of Tab. 1 were analyzed in [6] using Ansoft's Designer (AD) that shows good agreement between both simulation results and our proposed model. Fig. 13 displays the reflection phase diagram resulting from equivalent circuit model and numerical simulation for fifth sample.

The eighth sample of Tab. 1 was previously designed and simulated by FDTD method in [10] for a GALI-LEO/GPS system. The simulation results were verified experimentally. Therefore, this sample is a good candidate to show the validity of proposed equivalent circuit model for practical designing. The reflection phases of eighth sample for proposed model and numerical simulation are plotted in Fig. 14.
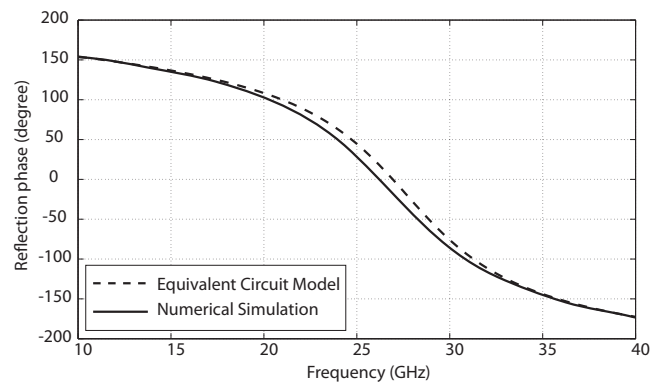
Fig. 13. The reflection phase diagram of sample 5 resulting from proposed model and numerical simulation.
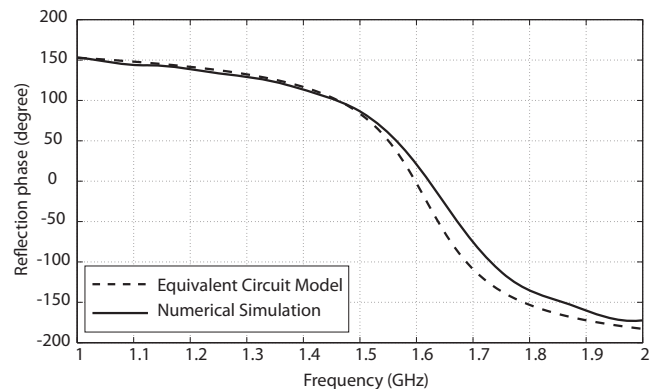
Fig. 14. The reflection phase diagram of sample 8 resulting from proposed model and numerical simulation.

In [11] the last sample of Tab. 1 was modeled by Transverse Equivalent Network (TEN) model. This structure was designed by one arm of JC-FSS. It is noted that, removing one arm of JC-FSS has no significant effect on the reflection phase feature. However, the non-symmetrical structure has different phase of reflection coefficient for TE and TM polarization. The reflection phases of this sample are shown in Fig. 15. It is observed that, the phase of reflection coefficient resulting from equivalent circuit model is very close to that using numerical simulation.
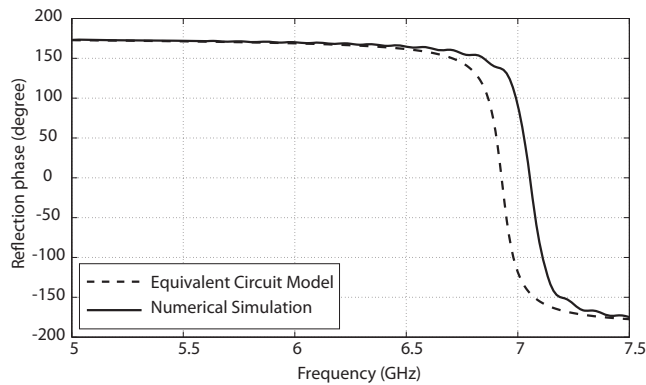
Fig. 15. The reflection phase diagram of sample 9 resulting from proposed model and numerical simulation.

5. Conclusion

The resonant frequency and reflection phase diagram of the Jerusalem cross-based artificial magnetic conductor have been estimated using an equivalent circuit model based on coupled microstrip lines and transmission line theories. To this aim, the characteristic impedance and the effective permittivity of the capacitive and inductive components of the JC-FSS element have been obtained separately. For normal incident wave to the surface of JC-AMC the accuracy of proposed model has been checked by designing many samples and the results have been validated by a numerical method. Design guidelines based on a comprehensive parametric study have also been discussed. Although this idea is proposed for the JC-based AMC structures, the model can be extended to other type of AMCs including different FSS shapes.

References

[1] SIEVENPIPER, D.F., ZHANG, L.J., BROAS, R.F.J., ALEXOPO-LOUS, N. G., YABLONOVITCH, E. High-impedance electromagnetic surfaces with a forbidden frequency band. *IEEE Trans. Microwave Theory & Techn.*, 1999, vol. 47, no. 11, p. 2059-2074.

[2] SIEVENPIPER, D. High-impedance electromagnetic surfaces. *Ph.D. dissertation*, Univ. Calif., Los Angeles, 1999.

[3] LUUKKONEN, O., SIMOVSKI, C., GRANET, G., GOUSSETIS, G., LIOUBTCHENKO, D., RAISANEN, A. V., TRETYAKOV, S. A. Simple and accurate analytical model of planar grids and high-impedance surfaces comprising metal strips or patches. *IEEE Trans. Antennas & Propag.*, vol. 56, no. 6, p. 1624 – 1632.

[4] SIMOVSKI, C. R., SOCHAVA, A. A. High-impedance surfaces based on self-resonant grids. Analytical modelling and numerical simulations. *Progress in Electromagnetics Research (PIER)* 2003, vol. 43, p. 239–256.

[5] ENGHETA, N., ZIOLKOWSKI, R. W. *Metamaterials: Physics and Engineering Explorations*. IEEE press published by Wiley-Interscience, 2006.

[6] HOSSEINI, M., HAKKAK, M. Characteristics estimation for Jerusalem cross-based artificial magnetic conductors. *IEEE Antenna and Wireless Propagation Letters*, 2008. vol. 7, p 58-61.

[7] SIMOVSKI, C. R., MAAGT, P. D., MELCHAKOVA, I. V. High-impedance surfaces having stable resonance with respect to

polarization and incidence angle. *IEEE Transaction on Antennas Propagation*, 2005, vol. 53, no. 3, p. 908-914.

[8] GUPTA, K. C., GARG, R., BAHL, I., BHARTIA, P. *Microstrip Lines and Slotlines*. 2nd ed. Norwood: Artech House, 1996.

[9] BAHL, I. *Lumped Elements for RF and Microwave Circuit*. Norwood: Artech House, 2003.

[10] BAGGEN, R., MARTINEZ-VAZQUEZ, M., LEISS, J., HOLZWARTH, S. Comparison of EBG substrates with and without vias for GALILEO/GPS applications. In *Proc. EuCAP 2007, 2nd European Conf. on Antennas and Propagation*. Edinburgh (UK), 2007.

[11] VALLECCHI, A., ALBANI, M., CAPOLINO, F. Planar metamaterial transverse equivalent network and its application to low-profile antenna designs. In *Proc. EuCAP 2009 – the 3rd European Conf. on Antennas and Propagation*. Berlin (Germany), 2009.

About Authors ...

Mirshahram HOSSEINIPANAH was born on September 13, 1971 in Tehran, Iran. He received the B.Sc. degree in communication engineering from Khaje Nasir Al-Deen Toosi University of Technology (KNTUT), Tehran, Iran in 1997 and the M.Sc. in medical radiation engineering from Sharif University of Technology (SUT), Tehran, Iran in 1999. In 1999, he joined the National Radiation Protection Dept. (NRPD) of Iran as a researcher in non-ionizing radiation engineering group. He has been awarded a scholarship by the government of China, Chinese Scholarship Council (CSC) and by the Ministry of Science, Research and Technology of Iran to do his PhD degree. He is currently working toward the PhD degree at School of Electronics and Information Engineering in Harbin Institute of Technology (HIT), Harbin, China. His research interests include artificial magnetic conductors, frequency selective surfaces, metamaterials, electromagnetic band-gap, antenna optimization and using analytical and numerical methods in microwave devices. He is a student member of the IEEE Microwave Theory and Techniques Society.

Qun WU was born on September 18, 1955 in Shang Zhi city, Heilongjiang Province, China. He obtained his B.Sc. degree in Radio Engineering, M. Eng. degree in Electromagnetic Fields and Microwave Technology, and Ph.D. degree in Communication and Information Systems Engineering, all at Harbin Institute of Technology (HIT), Harbin, China in 1977, 1988, and 1999, respectively. He worked as a Visiting Professor at Seoul National University (SNU) in Korea, from 1998 to 1999, and Pohang University of Science and Technology, from 1999 to 2000. Since 1990, he has been with Dept. of Electronic and Communication Engineering at HIT, China, where he is currently a Professor. He received two Third-Class Prizes and one Second-Class Prize of Scientific Progress Awards from the Ministry of Aerospace of China in 1989 and 1992, respectively. Dr Wu has published over 100 international and regional refereed journal papers. His recent research interests are mainly in microwave active circuits. He is a senior member of IEEE Microwave Theory and Techniques society and vice president of IEEE Harbin section.